ORIGINAL RESEARCH

HMGB1 Expression Levels Correlate with Response to Immunotherapy in Non-Small Cell Lung Cancer

Maria González-Cao[1], Xueting Cai[2], Jilian Wilhelmina Paulina Bracht [ID][3], Xuan Han[2], Yang Yang[2], Carlos Pedraz-Valdunciel[4], Teresa Morán[5], Javier García-Corbacho[6], Andrés Aguilar[1], Reyes Bernabé [ID][7], Pedro De Marchi[8,9], Luciane Sussuchi da Silva [ID][8], Leticia Ferro Leal[8], Rui Manuel Reis [ID][8,10,11], Jordi Codony-Servat[4], Eloisa Jantus-Lewintre [ID][12–14], Miguel Angel Molina-Vila[4], Peng Cao[2,15], Rafael Rosell [ID][1,16]

[1]Translational Cancer Research Unit, Instituto Oncológico Dr Rosell, Dexeus University Hospital, Barcelona, Spain; [2]Integrated Traditional Chinese and Western Medicine Department of Affiliated Hospital, Nanjing University of Chinese Medicine, Nanjing, Jiangsu, People's Republic of China; [3]Amsterdam University Medical Center (UMC), Amsterdam, The Netherlands; [4]Laboratory of Oncology, Pangaea Oncology, Quirón Dexeus University Hospital, Barcelona, Spain; [5]Medical Oncology Department, Catalan Institute of Oncology (ICO), Germans Trias i Pujol Hospital, Badalona, Spain; [6]Medical Oncology Department (Hospital Clinic)/Translational Genomics and Targeted Therapies in Solid Tumors (IDIBAPs), Barcelona, Spain; [7]Medical Oncology Department, Hospital Universitario Virgen del Rocío, Sevilla, Spain; [8]Molecular Oncology Research Center; Barretos Cancer Hospital, Barretos, Brazil; [9]Oncoclinicas, Rio de Janeiro, Brazil; [10]Life and Health Sciences Research Institute (ICVS), School of Medicine, University of Minho, Braga, Portugal; [11]ICVS/3b's – PT Government Associate Laboratory, Braga/Guimarães, Portugal; [12]Valencian Community Foundation Principe Felipe Research Center, Laboratory of Molecular Oncology, Valencia, Spain; [13]Centro de Investigación Biomédica en Red (CIBERONC), Madrid, Spain; [14]Universitat Politècnica de Valencia, Biotechnology Department, Valencia, Spain; [15]College of Pharmacy, Nanjing University of Chinese Medicine, Nanjing, Jiangsu, People's Republic of China; [16]Laboratory of Molecular Biology, Germans Trias i Pujol Health Sciences Institute and Hospital (IGTP), Badalona, Spain

Correspondence: Rafael Rosell, Laboratory of Molecular Biology, Germans Trias i Pujol Health Sciences Institute and Hospital (IGTP), Camí de les Escoless/n, Badalona, Barcelona, 08916, Spain, Tel +34 930330520, Email rrosell@iconcologia.net; Peng Cao, College of Pharmacy, Nanjing University of Chinese Medicine, Nanjing, 210023, People's Republic of China, Tel +86 85608666, Email cao_peng@njucm.edu.cn

Purpose: High-mobility group box 1 protein (HMGB1) is subject to exportin 1 (XPO1)-dependent nuclear export, and it is involved in functions implicated in resistance to immunotherapy. We investigated whether HMGB1 mRNA expression was associated with response to immune checkpoint inhibitors (ICI) in non-small cell lung cancer (NSCLC).

Patients and Methods: RNA was isolated from pretreatment biopsies of patients with advanced NSCLC treated with ICI. Gene expression analysis of several genes, including HMGB1, was conducted using the NanoString Counter analysis system (PanCancer Immune Profiling Panel). Western blotting analysis and cell viability assays in EGFR and KRAS mutant cell lines were carried out. Evaluation of the antitumoral effect of ICI in combination with XPO1 blocker (selinexor) and trametinib was determined in a murine Lewis lung carcinoma model.

Results: HMGB1 mRNA levels in NSCLC patients treated with ICI correlated with progression-free survival (PFS) (median PFS 9.0 versus 18.0 months, P=0.008, hazard ratio=0.30 in high versus low HMGB1). After TNF-α stimulation, HMGB1 accumulates in the cytoplasm of PC9 cells, but this accumulation can be prevented by using selinexor or antiretroviral drugs. Erlotinib or osimertinib with selinexor in EGFR-mutant cells and trametinib plus selinexor in KRAS mutant abolish tumor cell proliferation. Selinexor with a PD-1 inhibitor with or without trametinib abrogates the tumor growth in the murine Lewis lung cancer model.

Conclusion: An in-depth exploration of the functions of HMGB1 mRNA and protein is expected to uncover new potential targets and provide a basis for treating metastatic NSCLC in combination with ICI.

Keywords: HMGB1, immunotherapy, non-small cell lung cancer, Lewis lung cancer murine model, K-Ras mutations

Introduction

Immune checkpoint inhibitors (ICIs), such as anti-programmed death 1 (PD-1) and programmed death ligand 1 (PD-L1) antibodies, are widely used in advanced non-small-cell lung cancer (NSCLC)[1] and in multiple other primary malignancies,

including cancers in individuals infected with human immunodeficiency virus type 1 (HIV1) infection.[2,3] In advanced NSCLC, ICIs are recommended as single agents for patients with high PD-L1 expression (tumor proportion score >50%).[4] Tumors with concurrent mutations in KRAS and TP53 represent about 25% of NSCLCs, but there are no different indications for these patients according to the molecular alterations.[5] Although 20% of patients treated with ICIs achieve durable tumor response or stabilization, most patients do not respond. Mechanisms of resistance to immunotherapy are not fully understood. Durable tumor response or stabilization (clinical benefit) is achieved in approximately 20% of ICI-treated patients.[6] A whole-exome and transcriptome analysis of over 1000 patients treated with ICI across seven tumors indicates that a munnion of ICI response predictors should be kept in mind.[7] We have focused our research on the potential role of HMGB1 as an immunoresistant mechanism in cancer cells. HMGB1 has different functions according its localization into nucleus, cytoplasm or extracellular. HMGB1 works in the nucleus as a nonhistone nucleoprotein and in the extracellular space as an inflammatory cytokine. Intracellular HMGB1 is involved in transcriptional regulation, DNA replication and repair, telomere maintenance, and nucleosome assembly. Extracellular HMGB1 functions as a cytokine and binds to pattern recognition receptors (PRRs) working as a damage-associated molecular pattern (DAMP). HMGB1 is translocated to the cytoplasm from the nucleus through the protein transport XPO1 formerly known as chromosome-region maintenance-1 (CRM1). In a previous clinical trial,[2] we demonstrated that cancer patients infected with HIV responded to durvalumab (anti-PD-L1 monoclonal antibody) without unexpected adverse events. Since Exportin-1 (XPO1) also facilitates the nuclear export of HIV RNA,[8] it is plausible to suggest that integrase inhibitors (INSTIs) might enhance ICI efficacy by preventing the nuclear export of several factors, including HMGB1 through XPO1. However, whether HMGB1 is dispensable for the nuclear export of multiple tumor suppressor proteins and cell cycle regulators, such as NFKB1A (IkBα), p53, p21, and E2F7, among others, is a matter that warrants investigation. Leptomycin-B has been noted to inhibit XPO1 by preventing interaction with the HMGB1 protein. Selinexor (formerly known as KPT-330), an oral reversible covalent inhibitor of XPO1 that has demonstrated broad anticancer activity in advanced solid tumors[9] and in refractory myeloma patients[10] has been shown to slow B16F10 melanoma tumor growth in combination with ICIs (anti-PD-1 or anti-CTLA4).[11] Also, KPT-330 was active in NSCLC cell lines with wild-type p53 (A549) and mutant p53 (PC14). KPT-330 treatment abolished CCDN1 and c-Myc expression in A549 and PC14 cancer cells.[12] In the current study, we performed gene expression analysis using the NanoString IO360 panel targeting 770 genes, including HMGB1, on pre-ICI therapy tumor tissue samples from both HIV-positive and HIV-negative NSCLC patients. The aim was to evaluate the prognostic value of HMGB1 mRNA. In addition, we analyzed the nuclear-cytoplasmic shuttling of HMGB1 protein and assessed selinexor activity in a panel of NSCLC cell lines. Furthermore, in vivo experiments using a Lewis lung cancer model were conducted to evaluate the activity of selinexor in combination with ICI (anti-PD-L1 monoclonal antibody) and trametinib (MEK inhibitor).

Material and Methods
Patients and Cell Lines
Formalin fixed paraffin-embedded (FFPE) pre-treatment tumor tissue samples and stored plasma samples from ICI-treated cancer patients were retrospectively collected from two patient cohorts: HIV-1 infected cancer patients from the DURVAST trial[2] and patients without HIV-1 from Hospital Universitari Dexeus (Tables 1 and S1). Additional information may be found in the Background and Rationale section and Methods section of the Supplementary Appendix. An external validation cohort was performed at Barretos Cancer Hospital, Barretos, Brazil, in tumor samples from 41 NSCLC patients treated with ICI (Table 1). This study was carried out in accordance with the principles of the Declaration of Helsinki under an approved protocol of the institutional review board of Quirón Hospitals. Written informed consent was obtained from all patients and documented; samples were de-identified for patient confidentiality. Treatment response was assessed using RECIST1.1 criteria. Clinical benefit was defined as the sum of patients with complete response (CR) or partial response (PR) plus stable disease (SD) longer than 24 weeks. Survival time was measured from the time of first anti-PD-1/PD-L1 administration to the time of tumor progression by RECIST 1.1 criteria or death. For overall survival (OS), median values were estimated with the use of Kaplan–Meier method. Summary statistics, frequency tables, and parametric and nonparametric statistical tests were used, as applicable. Statistical analyses were performed with the use of Prism software V8.4.3.

Table 1 Patient Characteristics

Characteristics	Discovery Cohort		Validation Cohort
	HIV-1 Infected (n = 15)	Non-HIV-1 Infected (n = 30)	Non-HIV-1 Infected (n=41)
Gender – no. (%)			
Male	12 (80.0)	17 (56.7)	26 (63)
Female	3 (20.0)	13 (43.3)	15 (37)
Age - yr			
Median	54	62	63
Range	30–73	47–82	38–80
Smoking status – no. (%)			
Never	2 (13.3)	1 (3.3)	6 (15)
Former/current	12 (80.0)	26 (86.7)	35 (85)
Unknown	1 (6.7)	3 (10.0)	0
Tumor type – no. (%)			
Lung*	12 (80.0)	29 (96.7)	41 (100)
Melanoma	2 (13.3)	0 (0.0)	0
Bladder	1 (6.7)	0 (0.0)	0
Mesothelioma	0 (0.0)	1 (3.3)	0
Stage – no. (%)			
Stage III	1 (6.7)	2 (6.7)	5 (12)
Stage IV	14 (93.3)	28 (93.3)	36 (88)
ICI Treatment – no. (%)			
Durvalumab	15 (100)	2 (6.7)	4 (10)
Nivolumab	0 (0.0)	18 (60.0)	19 (46)
Pembrolizumab	0 (0.0)	5 (16.7)	11 (27)
Atezolizumab	0 (0.0)	3 (10.0)	4 (10)
Others	0 (0.0)	2 (6.7)	3 (7)
Treatment Regimen – no. (%)			
Single	15 (100)	19 (63.3)	19 (46)
With chemotherapy	0 (0.0)	5 (16.6)	13 (32)
Other combination	0 (0.0)	6 (20.1)	9 (22)
No. of prior systemic therapies – no. (%)			
0	8 (53.3)	12 (40.0)	24 (58)
1	4 (26.7)	14 (46.7)	7 (17)
≥ 2	3 (20.0)	4 (13.3)	10 (24)

(*Continued*)

Table 1 (Continued).

Characteristics	Discovery Cohort		Validation Cohort
	HIV-1 Infected (n = 15)	Non-HIV-1 Infected (n = 30)	Non-HIV-1 Infected (n=41)
cART – no. (%)			
NRTIs + INSTIs	12 (80.0)	0 (0.0)	0
NRTIs + non-INSTIs	3 (20.0)	0 (0.0)	0

Notes: *Lung cancer histology in the discovery cohort: adenocarcinoma 31 (69%), squamous carcinoma 8 (18%), small cell lung cancer 8 (18%); lung cancer histology in the validation cohort: adenocarcinoma 26 (63%), squamous 14 (34%), adeno-squamous 1 (2%).
Abbreviations: c ART, combination antiretroviral therapy; NRTIs, nucleoside reverse transcriptase inhibitors; ICI. Immune check point inhibitor; INSTIs, integrase strand transfer inhibitors; yr, year.

Chemicals and Reagents

Selinexor (S7252), raltegravir (S2005), elvitegravir (S2001), dolutegravir (S2667) and osimertinib (AZD9291, S7297) were purchased from Selleck, China. Erlotinib (HY-50896) and the MEK inhibitor (HY-12202) were purchased from MedChemExpress, China. Anti-mouse PD-L1 (Catalog number: BE0101) and polyclonal rat IgG (Catalog number: BE0094) were purchased from Bio X Cell (New Hampshire, USA). TNF-α and LPS were purchased from Sigma-Aldrich (St. Louis, MO, USA). The antibodies against the following proteins were used: HMGB1 polyclonal antibody (catalog number: ab167718, lot number: GR309540-1) (Abcam, Cambridge, MA, USA); Lamin B1 polyclonal antibody (catalog number: AP6001, lot number: AAD45161) and GAPDH polyclonal antibody (catalog number: AP0063, lot number: AA0118J1908N0063) (Bioworld Technology, Nanjing, China). The following secondary antibody was used: anti-rabbit IgG (H+L) (DyLight 800 4X PEG Conjugate) (catalog number: 5151, lot number: 12) (Cell Signaling Technology, Beverly, MA, USA). H520, PC9, A549, H1975 and Lewis lung carcinoma cells (LLC) cell lines were purchased from the American Type Culture Collection (ATCC). All cell lines were maintained in RPMI (Roswell Park Memorial Institute Medium) 1640 supplemented with 1% penicillin/streptomycin/glutamine (Gibco) and 10% fetal bovine serum (FBS; Gibco) in a 5% CO_2 37°C cell culture incubator and routinely evaluated for mycoplasma contamination.

Extracellular Vesicle Enrichment

The miRCURY® Exosome Serum/Plasma Kit (Qiagen, Hilden, Germany) was used to enrich EVs from 500 μL plasma, according to the manufacturer's instructions and as described previously.[13] Samples were incubated overnight at 4°C, and the EV-enriched fractions were pelleted by centrifugation. EV enriched pellets were resuspended for further processing.

RNA Isolation and Gene Expression Analysis Using nCounter

FFPE slides (5 μM) of pre-treatment tumor biopsies were stained with hematoxylin and eosin. The tumor area was evaluated by a pathologist, and samples were macro-dissected. RNA extraction and gene expression analysis using the NanoString nCounter platform with the Human PanCancer IO360 code set (NanoString Technologies Inc., Seattle, WA, USA) were carried out as published previously.[2] In addition, EV-enriched pellets were treated with 4 μg/mL RNase A (Sigma-Aldrich, St. Louis, MO) for 1 h at 37°C, to remove extracellular RNA not associated with EVs. Tri-reagent (MRC, Cincinnati, OH) was used for RNA extraction and RNA was pre-amplified, as published previously.[13] The IO360 panel was then used to analyze the expression of 770 genes related to tumor biology, immune response and micro-environment. In addition, the IO360 panel contains gene signatures to measure immune cell populations and tumor and immune activities. Samples were hybridized for 18 h at 65°C.

Data Normalization and Differential Expression Analysis

Raw reporter counts were preprocessed using the nSolver Analysis Software version 4.0 (NanoString Technologies Inc.). An initial quality control step was performed for each sample, and counts were then normalized for technical assay variation,

sample input variability, and background noise. Data analysis was performed on log2-transformed data using R and R-studio version 3.5.3. Fold change in expression of each gene between the two groups was calculated based on the average gene expression of each group. Appropriate statistical testing was performed within the software to determine differentially expressed genes (DEGs) between groups, and nominal p-values have been reported. Fold changes and p-values were depicted in volcano plots for visualization, where a fold change of 1 and nominal p-value of <0.05 was used to define DEGs. Differences between responder and non-responder cohorts were determined using a Mann–Whitney U-test.

NGS for Mutation Testing

DNA was isolated from either tissue or plasma samples of all patients, and next-generation sequencing (NGS) was performed with the GeneReader Platform (Qiagen, Hilden, Germany), as described previously.[13]

ELISA Analysis

Levels of HMGB1 protein in plasma from cancer patients (n=30) were assessed by ELISA with the Human High Mobility Group Protein B1 (HMGB1) ELISA kit (Abbexa, Cambridge, UK) following manufacturer's instructions. Plasma samples were diluted 1:100 due to the range of the ELISA kit (15.5 pg/mL-1000 pg/mL). The absorbance values were observed at 450 nm. The results were expressed as nanograms of protein per milliliter of plasma. The Mann–Whitney test was performed using Prism 9 software (GraphPad, Dotmatics, Boston, USA). Significance was set at $P < 0.05$ for all statistical tests.

Cell Viability Assays

The cell viability was determined using the Cell Counting Kit-8 assay (Med Chem Express, NJ, USA). Briefly, cells in the logarithmic phase were seeded at a density of 70 ~ 80% confluence per well in 96-well plates at 37°C with 5% CO2 for overnight incubation and treated with appropriate concentrations of test samples for the indicated times. After treatment, 10 μL of CCK-8 solution was added to each well and incubated at 37°C for 2 h. The absorbance was measured by Multiskan Spectrum Microplate Reader (Thermo Fisher Scientific, USA) at 450 nm.

Western Blotting

For Western blot analysis, total protein was prepared from cells by using RIPA lysis buffer (Beyotime, China). Proteins from the nucleus and cytoplasm were separated by NE-PER nuclear and cytoplasmic extraction reagents (Pierce, USA) and measured using the Nanodrop 1000 Spectrophotometer (Thermo Fisher Scientific, USA).

The equivalent amounts of protein were subjected to sodium dodecyl sulfate polyacrylamide gel electrophoresis (SDS-PAGE) and then transferred to nitrocellulose membranes. After blocking with 5% non-fat milk solution for 2 h at room temperature, the membranes were washed with TBS-Tween-20 (0.1%, v/v) and then incubated with primary antibody at 4°C overnight. Membranes were then incubated with horseradish peroxidase-conjugated anti-rabbit and anti-mouse antibodies at room temperature for 2 h and scanned using an Odyssey infrared fluorescence scanner (LI-COR Biosciences, Lincoln, NE, USA).

In vivo Experiments

C57BL/6 male mice (20 ± 2 g, 5–6-month-old) were obtained from Jiangsu Huachuang Sino Pharmaceutical Technology Co., Ltd. (Taizhou, Jiangsu, China). All animals were maintained in a clean facility in Jiangsu Province Academy of Traditional Chinese Medicine (Nanjing, Jiangsu, China). Mice were kept in cages with free access to food and water, at 20°C and 50 ± 20% relative humidity under a 12:12 h light: dark cycles and pathogen-free conditions. All procedures were based on the Guide for Care and Use of Laboratory Animals of National Institutes of Health and approved by Institutional Animal Care and Use Committee of Jiangsu Province Academy of Traditional Chinese Medicine (SYXK 2021–0025).

A suspension of 5×10^5 Lewis lung carcinoma cells resuspended in PBS was injected subcutaneously into the right flank of mice (Day 0). When established tumors become palpable (Day 8), mice were randomized into model group, vehicle (2% DMSO+40% PEG300+5% Tween 80 in ddH$_2$O, intragastric (*i.g.*)) + Isotype group (10 mg/kg IgG in PBS, intraperitoneal injection (*i.p.*)), selinexor (15 mg/kg in vehicle, *i.g.*) + Isotype group, trametinib (1.5 mg/kg in vehicle, *i.g.*) + Isotype group, Vehicle + PD-L1 mAb group (10 mg/kg in PBS, *i.p.*), selinexor + PD-L1 mAb group, selinexor + PD-L1 mAb + trametinib group. Selinexor and PD-L1 mAb treatments were administered once every three days. Trametinib treatments were

administered every day (Day 8–19). The body weight and tumor size were measured once every three days. Tumor volume was calculated as follows: length × (width^2) × 0.5. At the end of the experiments (Day 20), all animals were sacrificed, and the tumors were excised and weighed.

Statistical Analysis

Independent *t*-tests were used to calculate nominal P-values and Fold Change in patients with and without clinical benefit. Log rank tests were used to compare the survival distributions of the included patients.

The experimental data obtained from cultured cells and mice were analyzed using the unpaired *t*-test and one-way ANOVA to determine the significance of the difference between the two groups and are presented as the mean ± SD from independent experiments. Western blotting analyses were repeated with three independent experiments, and the results were quantified using ImageJ software. Statistical analysis was carried out using GraphPad Prism 8.0.1 software. A value of $P < 0.05$ was considered significant.

Results

Low HMGB1 mRNA Expression Could Be a Prognostic Factor

We analyzed HMGB1 mRNA expression on formalin-fixed paraffin embedded (FFPE) tumor tissue samples from pre-ICI treated cancer patients, both HIV-1 infected and non-infected (Table 1, Figure S1A). Table 1 displays the characteristics of the exploratory cohort of patients, while Table S1 shows the genetic alterations identified by NGS. Notably, none of the 45 patients harbor EGFR mutations, although KRAS mutations were frequently observed, often in combination with TP53 mutations. Additionally, several patients exhibited copy number gains, with MET amplification being the most common. Differential gene expression analysis revealed a cluster of significantly dysregulated genes in patients without clinical benefit from ICI treatment (p<0.05 and >2-fold change, Figure 1).
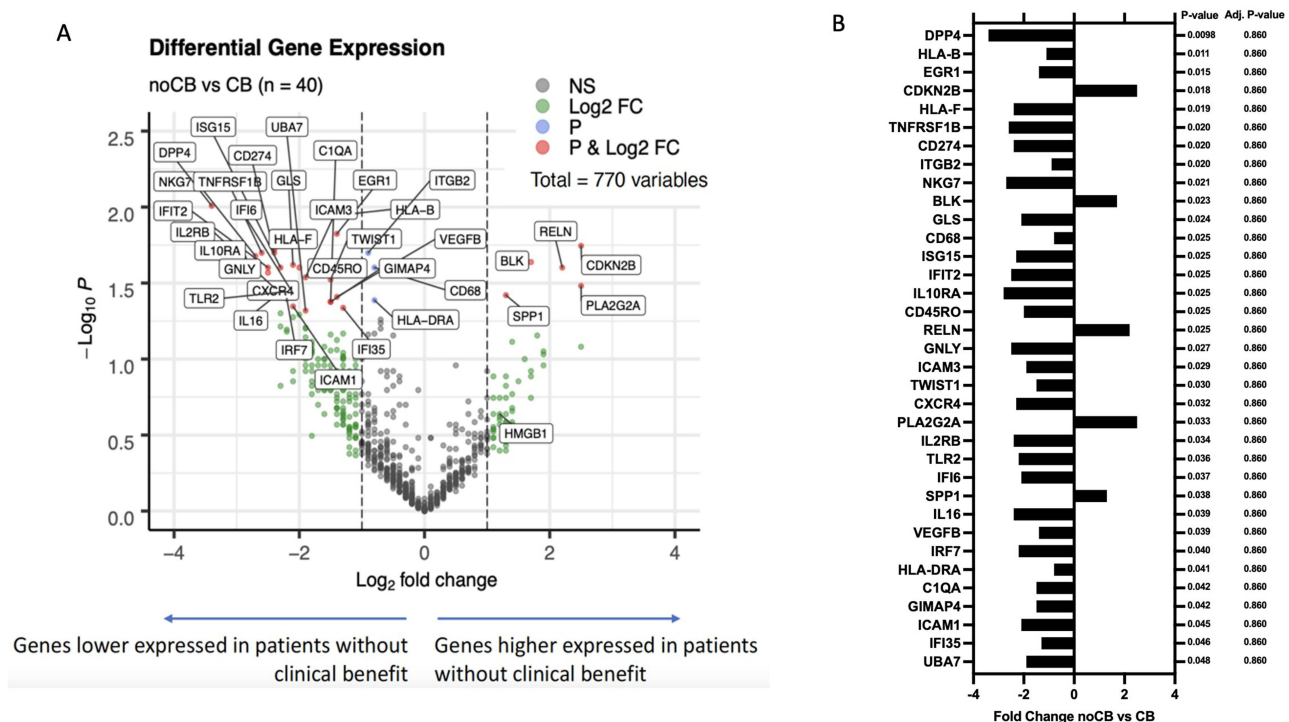

Figure 1 HMGB1 mRNA expression in pre-ICI-treatment FFPE tumor tissue samples. (**A**) Volcano plot indicating differential expression of the genes included in the IO360 panel. Genes depicted in green indicate a log2 Fold Change > 1, genes depicted in blue indicate a nominal p-value < 0.05, genes depicted in red indicate a log2 Fold Change > 1 and a p-value < 0.05. (**B**) Significantly differentially expressed genes between patients with and without clinical benefit, based on the Fold Change and nominal p-value (independent *t*-test). P-values adjusted for multiple testing are also included.
Abbreviations: CB, clinical benefit; ns, not significant; Adj. P-value, adjusted P-value.

In addition, HMGB1 mRNA was higher in patients without clinical benefit from ICI treatment compared to those with clinical benefit (n=40, p=0.048, Figure S1B). Other differentially expressed genes included CD274 (encoding PD-L1) and several transcripts related to the human leukocyte antigen (HLA) complex (Figures 1A, B, S2A and S2B). For 31 patients, stored plasma samples were available, and extracellular vesicle-mRNA expression was analyzed on the nCounter platform using the previously mentioned gene panel. As a result, an average of 212 transcripts out of the 770 genes included in the panel could be identified (Figure S3A). However, no counts above background were scored for HMGB1, indicating no expression of this gene in extracellular vesicles (EVs) of these patients (Figure S3B).

Protein-level screening of HMGB1 in plasma samples using enzyme-linked immunosorbent assay (ELISA) revealed measurable concentrations in all subjects assessed, ranging from 0.42 to 33.22 ng/mL. However, no differences were observed in patients without clinical benefit from ICI treatment compared to those with clinical benefit (Figure S4), suggesting that the value as a prognostic factor of HMGB1 is related to the intracellular fraction of the molecule and not to its extracellular fraction in plasma.

Low HMGB1 mRNA Expression Correlates with Improved Overall Survival

Kaplan–Meier analysis showed that patients with lower HMGB1 mRNA expression in the exploratory cohort had a median overall survival of 18 months, compared to 9 months in those with high HMGB1 pretreatment levels (n=42, p=0.004, hazard ratio=0.30) (Figure 2A).

The prognostic value of HMGB1 levels was validated in samples from an external Brazilian cohort of 41 NSCLC patients treated with ICI, with a median overall survival of 35.5 months versus 18 months (p=0.023; hazard ratio=0.39) (Figure 2B). To evaluate the prognostic significance of HMGB1 expression in comparison to established markers, we conducted survival analyses for CD274 (PD-L1) RNA expression, assessed by nCounter, and PD-L1 expression, evaluated through immunohistochemistry (Figure S5A). All three markers were significantly differentially expressed between patients with and without clinical benefit, with HMGB1 mRNA expression showing the best separation in the survival curves (Figure S5B). In addition, no correlation was found between HMGB1 and PD-L1 expression at the transcriptional level (Spearman's $r = -0.267$, p = 0.076, Figure S5C), suggesting that the prognostic value of HMGB1 expression was independent of PD-L1 expression levels.

Selinexor and INSTIs Reduce Cytoplasmic HMGB1 in PC9 Cell Line

Since XPO1 inhibitors can prevent the release of HMGB1 from the nucleus to the cytoplasm, adding selinexor to other cancer treatments lowers HMGB1 in the cytoplasm and this effect may improve the therapy response. We investigated the effect of selinexor and antiretroviral drugs (INSTIs: dolutegravir, elvitegravir and raltegravir) on HMGB1 nuclear
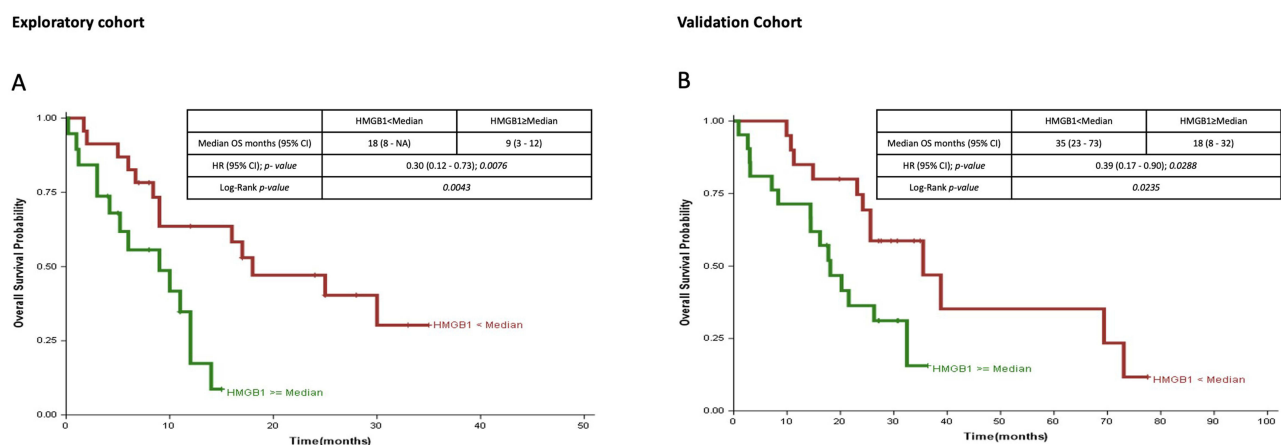

Figure 2 Overall survival (OS) analysis according to HMGB1 mRNA expression levels (lower versus higher that the median value). (**A**) In the exploratory cohort (n=42), there was a significant difference in overall survival for patients with low HMGB1 versus high HMGB1 mRNA expression level (hazard ratio [HR], 0.30; 95% CI, 0.12–0.73; *P*=0.0076) (**B**) In the validation cohort (n=41), a significant difference in overall survival was confirmed for patients with low versus high HMGB1 mRNA expression level (HR, 0.39; 95% CI, 0.17–0.90; *P*=0.0288).

export using the PC9 lung cancer cell line. Nuclear export of HMGB1 was induced using treatment with TNF-α for different time intervals. Cell nuclear and cytoplasmic protein were separated, and the HMGB1 level in total protein extracts was detected by Western blot. The results showed that TNF-α did not change the level of total HMGB1 within 8h, but it increased the HMGB1 levels in the cytoplasm, due to the increase in its nuclear export (Figure 3A).

To explore if the XPO1 inhibitor (selinexor) and/or INSTIs antiretroviral drugs can prevent the TNF-α induced nuclear export of HMGB1, PC9 cells were pre-treated with selinexor or INSTIs for 30 minutes. Cells were then exposed to TNF-α for 8 hours (Figure 3B). The Western blot analysis of proteins extracted from the nucleus and cytoplasm revealed that pre-treatment with selinexor or INSTIs reduced TNF-α-induced HMGB1 nuclear export.

Selinexor and Antiretroviral Drugs Inhibit Cell Proliferation in Lung Cancer Cell Lines

To determine the effect of HMGB1 nuclear retention, or depletion, on cell proliferation, we treated a panel of four lung cancer cell lines (H520, PC9, A549 and H1975) with selinexor and INSTIs (Figure 4A). Our results show that single selinexor treatment has an inhibitory effect on cell proliferation in all cell lines. When treating the cell lines with single INSTIs, elvitegravir showed better efficacy in inhibiting cell proliferation compared to dolutegravir and raltegravir. We tested the combined inhibitory effect of selinexor plus erlotinib or osimertinib in the EGFR-mutant H1975 and PC9 cell lines (Figure 4B and C, respectively). Combined EGFR inhibition and selinexor treatment lowered the cell viability compared to either treatment alone. Effects on cell viability after single or combined MEK inhibition and selinexor treatment were also tested in the KRAS-mutant A549 and H460 lung cancer cell lines (Figure 4D and E, respectively).
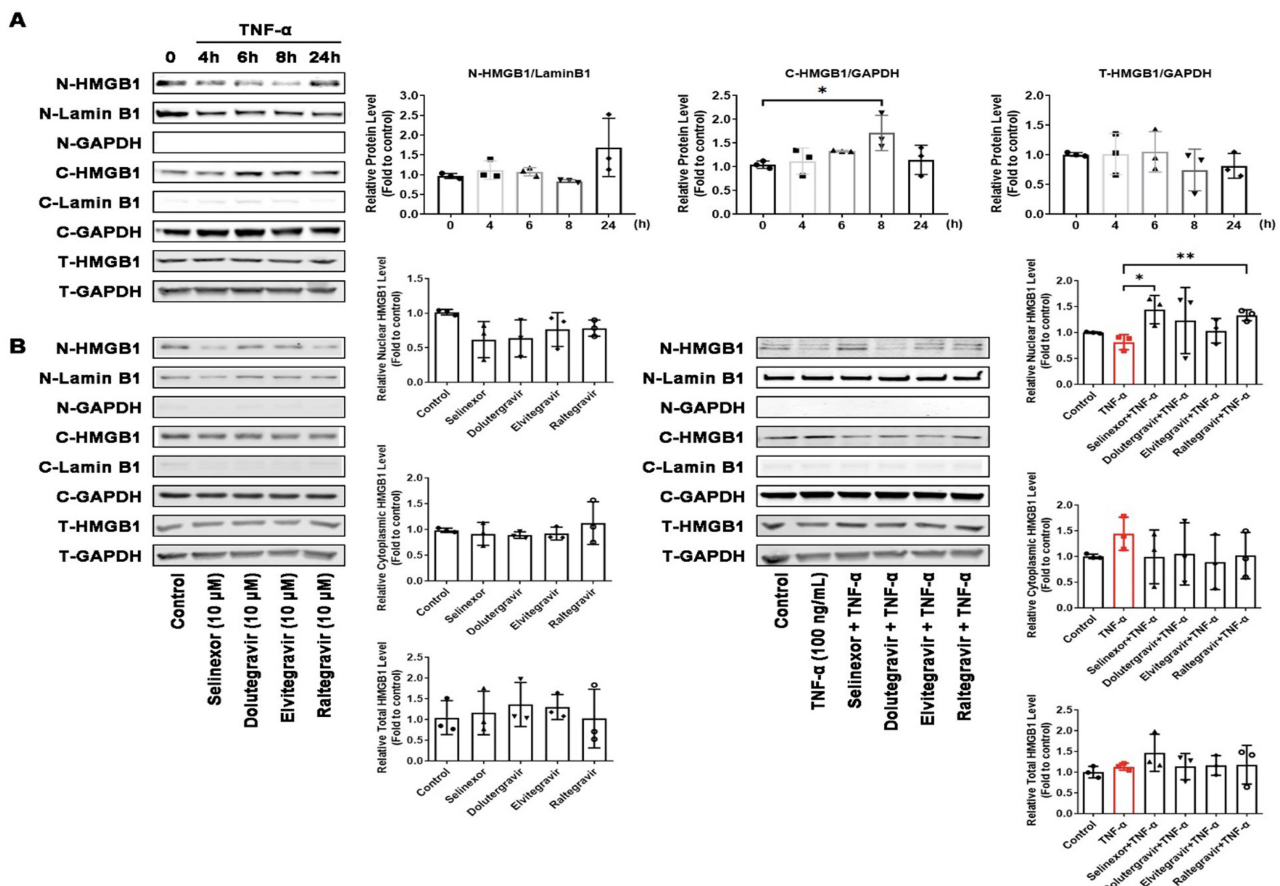

Figure 3 Effect of antiretroviral and selinexor treatment on nuclear export of HMGB1 in the PC9 cell line. (**A**) PC9 cells were treated with TNF-A (100ng/mL) to induce nuclear export of HMGB1, using different time intervals. Proteins from the nucleus and cytoplasm were separated and HMGB1 was detected by Western blotting. (**B**) PC9 cells were pre-treated with selinexor or antiretroviral drugs for 30 minutes and cells were then exposed to TNF-A (100 ng/mL) for 8 hours. Proteins from the nucleus and cytoplasm were separated and HMGB1 was detected by Western blotting. Data were analyzed using unpaired *t*-test comparisons.*P <0.05, **P <0.01, comparison between two groups marked with horizontal lines.

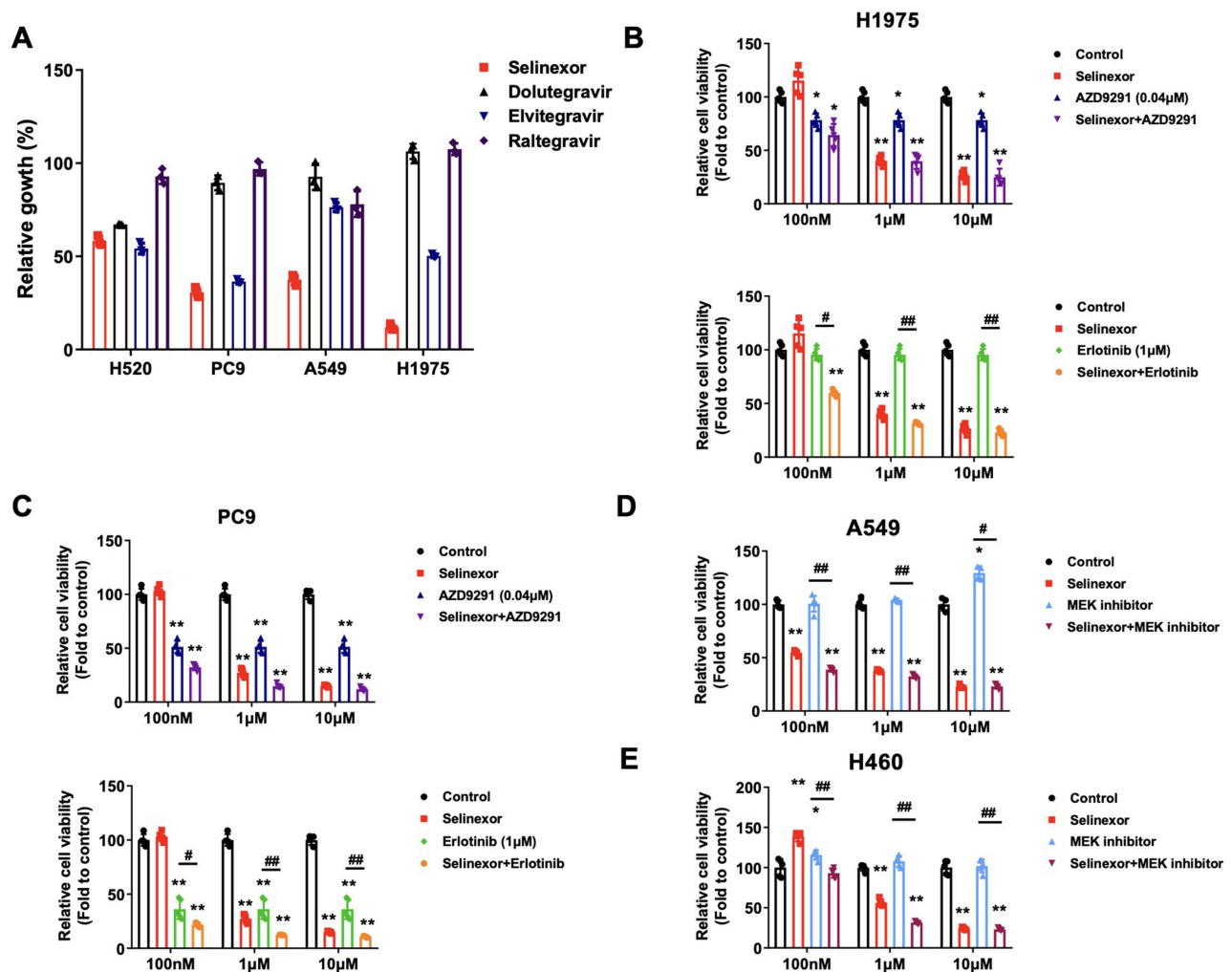**Figure 4** Effect of antiretroviral and selinexor treatment on cell viability analyzed by Cell Counting Kit-8 assay. (**A**) Effect of 20 uM single selinexor or antiretroviral treatments on cell viability in the H520, PC9, A549 and H1975 lung cancer cell lines, compared to the control. (**B**) Effect of single and combined selinexor plus osimertinib or erlotinib treatment on cell viability in the H1975 cell line, using different concentrations of selinexor. (**C**) Effect of single and combined selinexor plus osimertinib or erlotinib treatment on cell viability in the PC9 cell line, using different concentrations of selinexor. (**D**) Effect of single and combined selinexor plus MEK-inhibition treatment on cell viability in the A549 cell line, using different concentrations of selinexor. (**E**) Effect of single and combined selinexor plus MEK-inhibition treatment on cell viability in the H460 cell line, using different concentrations of selinexor. Data were analyzed using unpaired t-test comparisons. $*P <0.05$, $**P <0.01$, compared to control. $^{\#}P <0.05$, $^{\#\#}P <0.01$, comparison between two groups marked with horizontal lines.

Again, addition of selinexor to a MEK inhibitor significantly decreased cell viability compared to MEK inhibition alone in both cell lines.

Combination of Selinexor, Anti-PD-L1 Antibody, and Trametinib in Mice Bearing Lewis Lung Cancer Tumor

To determine whether selinexor can potentiate the MEK inhibitor and the ICIs treatment in vivo, combinatorial treatment of selinexor, PD-L1 mAb, and trametinib was performed in the LLC subcutaneous transplanted murine lung tumor model in vivo (Figure 5A). Subcutaneous transplanted tumor models help to quickly evaluate the effects of the drug combination. In future studies, we plan to establish lung cancer cells with luciferase to determine the efficacy of the drug combinations more accurately. The results showed that LLC tumor volumes in selinexor + isotype group were significantly larger than in selinexor + PD-L1 mAb group (p < 0.05). Furthermore, tumors in selinexor + PD-L1 mAb + trametinib group gradually vanished by the end point dissection (Figure 5B). During the treatment stage, mice's body weight did not show any significant change between each group (Figure 5C). On Day 20, the subcutaneous transplanted
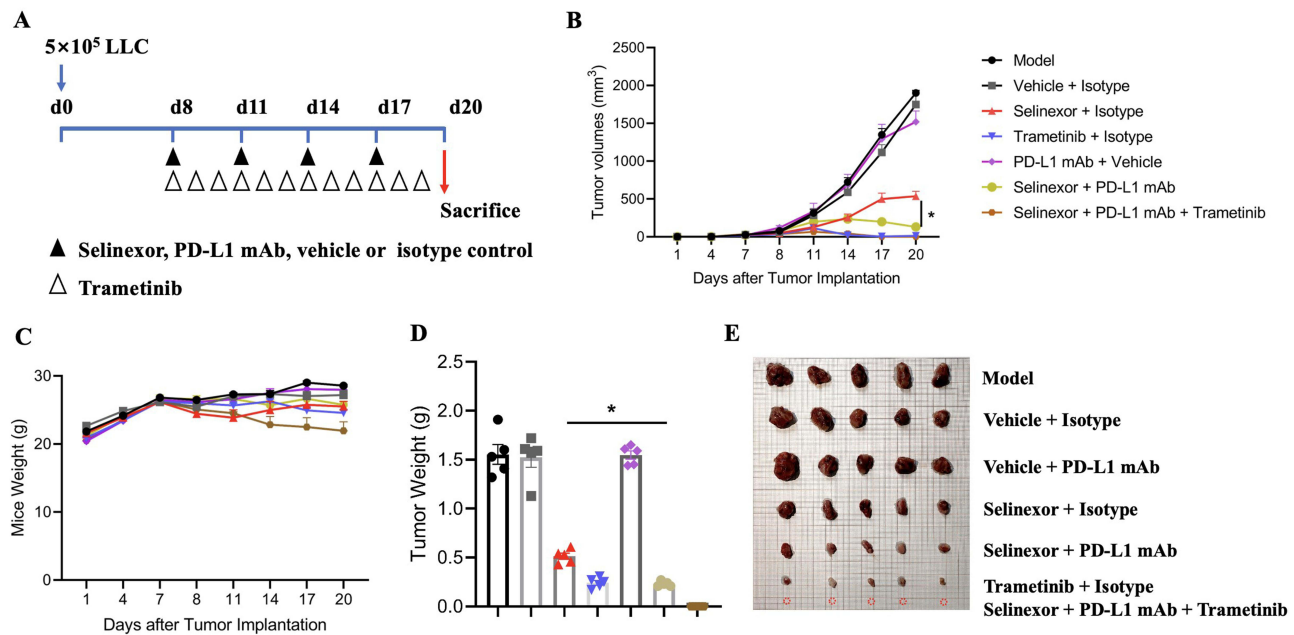
Figure 5 Anti-tumor efficacy of PD-L1 mAb in combination with selinexor and trametinib in vivo. (**A**) Time schedule for the LLC subcutaneous implantation and drug treatment groups, mice were randomly grouped into 7 groups: Model group, Vehicle + Isotype group, selinexor + Isotype group, trametinib + Isotype group, PD-L1 mAb + Vehicle group, selinexor + PD-L1 mAb group, and selinexor + PD-L1 mAb + trametinib group. (**B**) Tumor volumes for subcutaneous LLC tumor. (**C**) Mice body weight in each group. (**D**) Subcutaneous tumor weight in each group. (**E**) Representative LLC tumor pictures. (n=5). Data were analyzed using one-way ANOVA comparisons. *P <0.05, compared to the selinexor + Isotype group. (Regarding the results in (**B** and **D**)), there is a certain measurement error in measuring the size of a subcutaneous tumor with caliper (**B**). In fact, the smaller the tumor, the greater the measurement error. The actual tumor weight (**D**) and pictures (**C**) excised from mice are more accurate and intuitive.

tumor was excised and weighed. The tumor weight in the selinexor + PD-L1 mAb group significantly declined compared to selinexor + isotype group (Figure 5D and E, p < 0.05). There is no significant difference between the trametinib treatment group and the selinexor + PD-L1 mAb + trametinib combination treatment group, possibly because the trametinib treatment group had a good effect at the current dose, and the tumor was very small; however, the tumor in the selinexor + PD-L1 mAb + trametinib combination treatment group completely disappeared. In the future, other models can be explored to compare the trametinib treatment group and the combination of selinexor+PD-L1 mAb +trametinib. Above all, selinexor increased the PD-L1 mAb treatment efficacy in vivo and the MEK inhibitor, trametinib, improved the selinexor + PD-L1 mAb combination, with complete regression of the LLC tumor in vivo.

Discussion

Checkpoint inhibition immunotherapy combined with chemotherapy has been shown to increase overall survival compared to chemotherapy alone, as demonstrated in clinical trials such as KEYNOTE-189[14] and CheckMate 9LA.[15] However, a significant portion of patients with non-small cell lung cancer (NSCLC) do not respond to this treatment approach, including those with KRAS G12C and STK11 co-mutations[16] as well as patients with EGFR-mutant NSCLC.[17,18] The mechanisms that produce resistance to immunotherapy are not fully known, and multiple factors could be involved. We have focused our research on exploring the role of HMGB1 as a possible factor of resistance to immunotherapy in NSCLC. Localization of HMGB1 into the nucleus, cytoplasm or extracellular spaces modifies its functions.[19] One possible mechanism of HMGB1's effect on cells could be related to its function when it is translocated from the nucleus to the cytoplasm upon cell activation or stress, where it is involved in inflammasome activation and pyroptosis, promoting autophagy and inhibiting apoptosis.[20] Different endogenous stimuli of the host origin, such as tumor necrosis factor alpha (TNFα), peroxynitrite, and others, can induce secretion of HMGB1.[21,22]

Using a targeted expression quantification assay (nCounter PanCancer IO360 panel), HMGB1 mRNA expression levels were unexpectedly found to be lower in HIV-1 infected cancer patients in contrast with non-HIV-infected patients (Log2 fold change −1.59, p < 0.01). Further assessment comparing such HIV-1 infected cancer patients treated with

durvalumab[2] and a group of NSCLC patients receiving immunotherapy as a second- or third-line treatment (Table 1) confirm HMGB1 mRNA levels as a prognostic factor of survival. Henceforth, the prognostic value of HMGB1 mRNA levels was confirmed in an independent series of Brazilian NSCLC patients treated with anti-PD-1 Ab. Previous studies have also found that high HMGB1 mRNA and protein levels in different types of tumors are a poor prognostic factor.

Inhibition of the HMGB1 transporter XPO1 with selinexor or INSTIs under TNF-α induction led to nuclear retention of HMGB1 in the PC9 cell line. It is of particular interest to further decipher mechanistically the contribution of HMGB1 in KRAS mutant NSCLC. KRAS is a G-quadruplex controlled oncogene[23] and HMGB1 binds and stabilizes the G-quadruplex of the KRAS promoter element responsible for the transcriptional activity.[24] Moreover, KRAS mutant NSCLC with STK11 co-mutation has increased expression of the autophagy-inducing kinase ULK1 (unc-51-like autophagy activating kinase 1), and ULK1 inhibition can enhance ICI effect.[25] Previous data have demonstrated the role of extracellular HMGB1 as a ligand of T-cell immunoglobulin mucin family member 3 (Tim-3) in dendritic cells.[26] However, the release of extracellular HMGB1 should not be ruled out as a mechanism of immune resistance. Our data do not support this hypothesis, as only HMGB1 cell levels, and not plasma levels nor HMGB1 in extracellular vesicles, correlated with survival in our study.

To explore the effects of nuclear HMGB1 retention or depletion on cell proliferation, we treated four lung cancer cell lines with selinexor or INSTIs. Although INSTIs were able to lower cell proliferation in most cell lines, single selinexor treatment was found to be even more effective. Combination treatments with selinexor yielded a significant decrease in cell viability in KRAS and EGFR mutant positive lung cancer cell lines when compared to single MEK or EGFR inhibition. In melanoma, upregulation of PD-L1 through HMGB1 could be therapeutically exploited through either inhibition of the HMGB1/IRF3/NF-kB pathway or with ICIs.[27] Selinexor induced responses in myeloma multiple,[10] in mantle cell lymphoma,[28] and reversed anthracycline resistance in head and neck squamous cell carcinomas.[29] Moreover, XPO1 inhibition, and therefore nuclear HMGB1 retention, can repress STAT3 activation.[27] Combined selinexor and ICI therapy led to a significant reduction in the tumor growth rate in a melanoma mice model,[11] as we have seen in the Lewis lung cancer model. However, other factors besides HMGB1 can be involved in cancer response through XPO1 inhibition.

In summary, preclinical experiments indicate that both selinexor and antiretroviral drugs can prevent HMGB1 cytoplasmic accumulation. In vitro and in vivo evidence demonstrates a therapeutic effect of combining selinexor with ICI. The study has several shortcomings, including a lack of investigation into the cooperative function of HMGB1 with XPO1, failure to examine the nuclear export of other vital tumor suppressor proteins, such as p53 and NFKB1A, and to explore whether antiretroviral drugs could serve as effective repurposing agents similar to the activity of selinexor. Additionally, the correlation between XPO1 and HMGB1 levels warrants further investigation. Our findings suggest that further research should be carried out in NSCLC patients harboring KRAS mutations, or other genetic alterations, to study the role of pharmacological modulation of HMGB1 as a mechanism for improving the effect of ICI therapy.

Conclusion

Our study found that HMGB1 mRNA expression levels are associated with survival in metastatic NSCLC treated with anti-PD-1 Ab, suggesting its potential role as a biomarker and therapeutic target.

Data Sharing Statement

Data sharing is not applicable to this article as no datasets were generated or analyzed during the current study.

Acknowledgments

the Public Ministry of Labor Campinas (Research, Prevention, and Education of Occupational Cancer). This work is in memory of the generous support provided by the late Julian Santamaría Valiño to the IOR Foundation.

Disclosure

References

1. Rosell R, González-Cao M. Cemiplimab monotherapy in advanced non-squamous and squamous non-small cell lung cancer. *Lancet*. 2021;397 (10274):557–559. doi:10.1016/S0140-6736(21)00196-3
2. González-Cao M, Morán T, Dalmau J, et al. Assessment of the feasibility and safety of durvalumab for treatment of solid tumors in patients with HIV-1 infection: the Phase 2 DURVAST Study. *JAMA Oncol*. 2020;6(7):1063–1067. doi:10.1001/jamaoncol.2020.0465
3. Uldrick TS, Gonçalves PH, Abdul-Hay M, et al. Assessment of the safety of pembrolizumab in patients with HIV and advanced cancer—a Phase 1 study. *JAMA Oncol*. 2019;5(9):1332–1339. doi:10.1001/jamaoncol.2019.2244
4. Hanna NH, Schneider BJ, Temin S, et al. Therapy for Stage IV non–small-cell lung cancer without driver alterations: ASCO and OH (CCO) joint guideline update. *J Clin Oncol*. 2020;38(14):1608–1632. doi:10.1200/JCO.19.03022
5. Brahmer JR, Govindan R, Anders RA, et al. The Society for Immunotherapy of Cancer consensus statement on immunotherapy for the treatment of non-small cell lung cancer (NSCLC). *J Immunother Cancer*. 2018;6(1):75. doi:10.1186/s40425-018-0382-2
6. Topalian SL, Hodi FS, Brahmer JR, et al. Safety, activity, and immune correlates of anti–PD-1 antibody in cancer. *N Engl J Med*. 2012;366 (26):2443–2454. doi:10.1056/NEJMoa1200690
7. Litchfield K, Reading JL, Puttick C, et al. Meta-analysis of tumor- and T cell-intrinsic mechanisms of sensitization to checkpoint inhibition. *Cell*. 2021;184(3):596–614.e514. doi:10.1016/j.cell.2021.01.002
8. Booth DS, Cheng Y, Frankel AD. The export receptor Crm1 forms a dimer to promote nuclear export of HIV RNA. *Elife*. 2014;3:e04121. doi:10.7554/eLife.04121
9. Gupta A, Saltarski JM, White MA, Scaglioni PP, Gerber DE. Therapeutic targeting of nuclear export inhibition in lung cancer. *J Thorac Oncol*. 2017;12(9):1446–1450. doi:10.1016/j.jtho.2017.06.013
10. Chari A, Vogl DT, Gavriatopoulou M, et al. Oral selinexor–dexamethasone for triple-class refractory multiple myeloma. *N Engl J Med*. 2019;381 (8):727–738. doi:10.1056/NEJMoa1903455
11. Farren MR, Hennessey RC, Shakya R, et al. The exportin-1 inhibitor selinexor exerts superior antitumor activity when combined with t-cell checkpoint inhibitors. *Mol Cancer Ther*. 2017;16(3):417–427. doi:10.1158/1535-7163.MCT-16-0498
12. Sun H, Hattori N, Chien W, et al. KPT-330 has antitumour activity against non-small cell lung cancer. *Br J Cancer*. 2014;111(2):281–291. doi:10.1038/bjc.2014.260
13. Bracht JWP, Gimenez-Capitan A, Huang CY, et al. Analysis of extracellular vesicle mRNA derived from plasma using the nCounter platform. *Sci Rep*. 2021;11(1):3712. doi:10.1038/s41598-021-83132-0
14. Rodríguez-Abreu D, Powell SF, Hochmair MJ, et al. Pemetrexed plus platinum with or without pembrolizumab in patients with previously untreated metastatic nonsquamous NSCLC: protocol-specified final analysis from KEYNOTE-189. *Ann Oncol*. 2021;32(7):881–895. doi:10.1016/j. annonc.2021.04.008
15. Reck M, Ciuleanu TE, Cobo M, et al. First-line nivolumab plus ipilimumab with two cycles of chemotherapy versus chemotherapy alone (four cycles) in advanced non-small-cell lung cancer: checkMate 9LA 2-year update. *ESMO Open*. 2021;6(5):100273. doi:10.1016/j. esmoop.2021.100273
16. Scharpf RB, Balan A, Ricciuti B, et al. Genomic landscapes and hallmarks of mutant RAS in human cancers. *Cancer Res*. 2022;82(21):4058–4078. doi:10.1158/0008-5472.CAN-22-1731
17. Qiao M, Jiang T, Liu X, et al. Immune checkpoint inhibitors in EGFR-mutated NSCLC: dusk or dawn? *J Thorac Oncol*. 2021;16(8):1267–1288. doi:10.1016/j.jtho.2021.04.003
18. Lu S, Wu L, Jian H, et al. Sintilimab plus bevacizumab biosimilar IBI305 and chemotherapy for patients with EGFR-mutated non-squamous non-small-cell lung cancer who progressed on EGFR tyrosine-kinase inhibitor therapy (ORIENT-31): first interim results from a randomised, double-blind, multicentre, Phase 3 trial. *Lancet Oncol*. 2022;23(9):1167–1179. doi:10.1016/S1470-2045(22)00382-5
19. Mukherjee A, Vasquez KM. Targeting chromosomal architectural HMGB proteins could be the next frontier in cancer therapy. *Cancer Res*. 2020;80 (11):2075–2082. doi:10.1158/0008-5472.CAN-19-3066
20. Andersson U, Yang H, Harris H. High-mobility group box 1 protein (HMGB1) operates as an alarmin outside as well as inside cells. *Semin Immunol*. 2018;38:40–48. doi:10.1016/j.smim.2018.02.011
21. Tripathi A, Pandey V, Sahu AN, Singh A, Dubey PK. Di-(2-ethylhexyl) phthalate (DEHP) inhibits steroidogenesis and induces mitochondria-ROS mediated apoptosis in rat ovarian granulosa cells. *Toxicol Res*. 2019;8(3):381–394. doi:10.1039/C8TX00263K
22. Tcyganov EN, Sanseviero E, Marvel D, et al. Peroxynitrite in the tumor microenvironment changes the profile of antigens allowing escape from cancer immunotherapy. *Cancer Cell*. 2022;40(10):1173–1189.e1176. doi:10.1016/j.ccell.2022.09.001
23. Singh K, Lin J, Lecomte N, et al. Targeting eIF4A-dependent translation of KRAS signaling molecules. *Cancer Res*. 2021;81(8):2002–2014. doi:10.1158/0008-5472.CAN-20-2929
24. Amato J, Madanayake TW, Iaccarino N, et al. HMGB1 binds to the KRAS promoter G-quadruplex: a new player in oncogene transcriptional regulation? *Chem Commun*. 2018;54(68):9442–9445. doi:10.1039/C8CC03614D

25. Deng J, Thennavan A, Dolgalev I, et al. ULK1 inhibition overcomes compromised antigen presentation and restores antitumor immunity in LKB1-mutant lung cancer. *Nat Cancer*. 2021;2(5):503–514. doi:10.1038/s43018-021-00208-6

26. Chiba S, Baghdadi M, Akiba H, et al. Tumor-infiltrating DCs suppress nucleic acid-mediated innate immune responses through interactions between the receptor TIM-3 and the alarmin HMGB1. *Nat Immunol*. 2012;13(9):832–842. doi:10.1038/ni.2376

27. Wang W, Chapman NM, Zhang B, et al. Upregulation of PD-L1 via HMGB1-activated IRF3 and NF-κB contributes to UV radiation-induced immune suppression. *Cancer Res*. 2019;79(11):2909–2922. doi:10.1158/0008-5472.CAN-18-3134

28. Ming M, Wu W, Xie B, et al. XPO1 inhibitor selinexor overcomes intrinsic ibrutinib resistance in mantle cell lymphoma via nuclear retention of IkappaB. *Mol Cancer Ther*. 2018;17(12):2564–2574. doi:10.1158/1535-7163.MCT-17-0789-ATR

29. Saenz-Ponce N, Pillay R, de Long LM, et al. Targeting the XPO1-dependent nuclear export of E2F7 reverses anthracycline resistance in head and neck squamous cell carcinomas. *Sci Transl Med*. 2018;10(447). doi:10.1126/scitranslmed.aar7223